

Evaluation of Electrochemical Impedance Properties of Anti-corrosion Films by Arc Thermal Metal Spraying Method

Hong-Bok Choe¹, Han-Seung Lee^{1,*}, Mohamed A. Ismail¹ and Mohd Warid Hussin²

¹ Department of Architectural Engineering, Hanyang University, 1271 Sa 3-dong, Sangrok-gu, Ansan 426-791, South Korea

² Construction Research Centre (UTM CRC), Faculty of Civil Engineering, Universiti Teknologi Malaysia, 81310 UTM Johor Bahru, Johor, Malaysia

*E-mail: ercleehs@hanyang.ac.kr

Received: 30 March 2015 / Accepted: 20 August 2015 / Published: 30 September 2015

Arc thermal metal spraying method (ATMSM) provides proven long term protective coating systems using zinc, aluminum and their alloys for steel structure in a marine environment. This paper focused on studying the effect of spraying metal type, and presence or absence of pore sealing agent on impedance properties of Arc Thermal Metal Spraying (ATMS) film. The results showed that the impedance property of ATMS film was significantly varied depending on whether the metal type applied pertains to the Zn or Al series. Also, the reaction system between the interface of ATMS film and electrolyte was analyzed by interpreting its equivalent circuit. Consequently, the representative equivalent circuits were presented as models to be applied on ATMS film according to metal type (Zn series, Al series) and the presence or absence of a pore sealing agent.

Keywords: arc thermal metal spraying film; anti-corrosion performance; electrochemical impedance spectroscopy; sacrificial anode reaction

1. INTRODUCTION

When a steel structure is exposed to a marine environment, its durability can be decreased, to the extent of collapse, because of corrosion. Therefore, for maintaining the durability of the steel structure, it is essential to apply an anti-corrosion coating to efficiently inhibit its corrosion.

Thus far, this issue has not been sufficiently addressed. Meanwhile, the two conventional anti-corrosion methods that have been used: heavy duty coating and hot dip galvanizing; have limitations with respect to long-term anti-corrosion performance. In the case of heavy duty coating, once flaking occurs, steel cannot be easily protected; moreover, this flaking can be prevented only by frequent re-coating, which entails high maintenance and management costs. On the other hand, hot dip galvanizing

has issues with size limitations of structural members for applying, thermal deformation of base steel and technical difficulties with respect to sufficient coating thickness [1-5].

To address these issues, the arc thermal metal spraying method (ATMSM) has recently been introduced and applied. In this method, metal wires composed of sacrificial anodic property are melted by an electric arc and sprayed on the steel surface by a stream of compressed air to form an anti-corrosion film. The Arc Thermal Metal Spraying (ATMS) film thus protects the steel structure from corrosion via the formation of robust oxidation products on the steel surface while the film itself undergoes “sacrificial” corrosion under humidity in ambient air or in marine environments [6-8].

Moreover, ATMSM does not exert thermal deformation on members as well as demonstrates easy field application and thickness control of the anti-corrosion film. As an anti-corrosion technique for steel, it also ensures an excellent anti-corrosion performance and has several significant advantages over the conventional anti-corrosion methods [9].

To evaluate the anti-corrosion performance of films prepared by ATMSM, a qualitative test based on visual assessment and a quantitative test based on an electrochemical technique have been employed. These tests are the copper accelerated salt spray (CASS) test and Tafel extrapolation method, respectively [9-15].

Previous studies have verified that ATMS films have a lower corrosion rate and higher polarization resistance, which contributes to better anti-corrosion performance as compared to the anti-corrosion films prepared by conventional methods. ATMS films demonstrate more stable and efficient anti-corrosion performance with increasing Al content. In particular, when metals with high corrosion tendency such as Mg or Zn are alloyed with Al, initial corrosion is accelerated by Mg or Zn, resulting in the rapid formation of oxidation products, which exhibits effects of protecting the corrosion of Al that is the anti-corrosion film, thus improving the overall anti-corrosion performance of the ATMS film. Consequently, the steel structure can be protected from corrosion for a prolonged time period. Because of the aforementioned reasons, ATMSM is superior to the conventional methods for producing anti-corrosion film [9, 15].

The polarization resistance of an ATMS film measured by the Tafel extrapolation method and its comparative analysis can explain corrosion resistibility of ATMS film respectively. However, this method has a limitation in terms of distinguishing the individual factors that contribute to resistance with respect to the corrosion reactions that occur between the electrolyte and ATMS film.

This study investigates this issue by measuring the impedance, which represents the corrosion resistibility at the interface between the electrolyte and ATMS film, by electrochemical impedance spectroscopy. By impedance measurements, it is aimed to understand the corrosion resistance factors depending on the anti-corrosion state of the ATMS film (spraying metal type, and presence or absence of pore sealing agent) and represent the total reaction system of an ATMS film by designing an equivalent circuit, reflecting the measurement results.

2. EXPERIMENTAL PROGRAM

2.1 Principle of the arc thermal metal spraying method

Fig. 1 depicts the principle of the ATMSM. First, two strands of a metal wire are separately

introduced in and transported through metal spraying equipment (driving roller and driving device); next, they are melted at the arc point. The melted spraying metal is then diffused by compressed air while it is cooled. The temperature of metal particles instantly decreases to room temperature at soon as they collide on the steel surface. This collision eliminates the thermal deformation of the steel surface, thereby forming a robust and stable porous film [15].

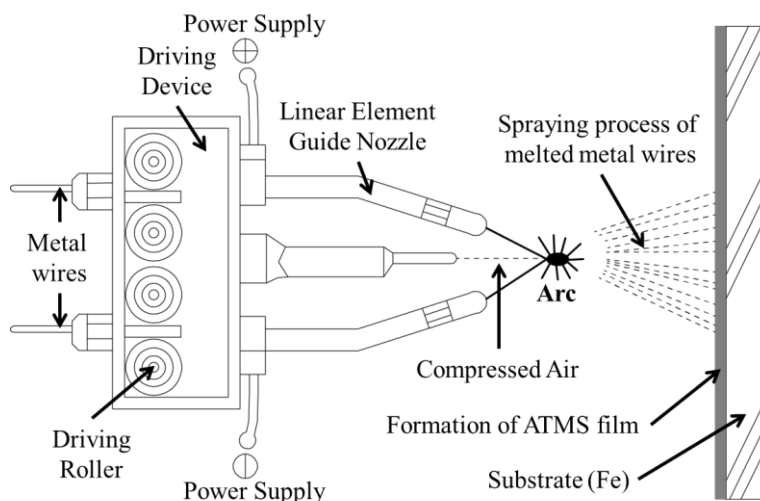


Figure 1. Principle of the arc thermal metal spraying method [15]

2.2 Test specimens for experiments

Table 1 gives an overview of the test specimens used in the EIS experiments. Specimen No. 1 is Substrate and No. 2 is anti-corrosion film prepared by conventional methods, hot dip galvanizing. Specimens No. 3 – No. 12 are those prepared by ATMSM.

To compare the impedance properties of the conventional and ATMS films, unpainted steel (US) as plain specimen and hot dip galvanizing (HDG) as the test specimen for the conventional anti-corrosion film were selected. To analyze and compare different metal wire types for ATMS films, Zn–Al, Zn–Sn (alloy), Al–Mg (alloy), Zn (single metal), and Al (single metal) were selected as these metals types have demonstrated excellent anti-corrosion performances in previous studies [9]. Specimen No.7 and No.8 are Zn–Al films used as a single spraying metal respectively which is not alloy; when used at the same volume ratio, the mass ratio was approximately 73% Zn and 27% Al.

Moreover, given that an ATMS film is generated in a stacked form of solid metal particles sprayed on a steel surface, it contains numerous pores between particles and around the surface. If moisture penetrates the film through the pores, corrosion occurs on the substrate. Therefore, one of the test variables was the presence or absence of an epoxy series coating as a pore sealing agent which retards the corrosion onset of an ATMS film and enhance its anti-corrosion performance. S and NS in the specimen names represent the presence and absence of a pore sealing agent, respectively.

The anti-corrosions methods were applied on the substrate SS41 (by JIS, chemical composition

is as follows; $C \leq 0.22\%$, $Mn \leq 1.4\%$, $Si \leq 0.35\%$, $S \leq 0.050$, $P \leq 0.045$), and the substrate surface was treated with sand blasting to ensure good adhesion between the ATMS film and substrate. The composition ratios of the metal wires were expressed in mass ratio, and the anti-corrosion thickness of the sprayed films was set at 100 μm , which is the average thickness applied in the construction industry.

Table 1. Details of the specimens used for the EIS experiments

| No. | Specimen Name ³ | Anti-Corrosion Method | Types of spraying metal [Alloy or Single metal] | Mass Ratio of metal | Usage of Pore Sealing Agent |
|-----|----------------------------|-------------------------|---|---------------------|-----------------------------|
| 1 | US ¹ | - | - | - | - |
| 2 | HDG ² | - | - | - | - |
| 3 | (Zn) – S ⁴ | Arc Thermal Metal Spray | (Zn) - (Zn) [Single metal] | Zn 100% | Yes |
| 4 | (Zn) – NS ⁵ | Arc Thermal Metal Spray | (Zn) - (Zn) [Single metal] | Zn 100% | No |
| 5 | (Al) – S | Arc Thermal Metal Spray | (Al) - (Al) [Single metal] | Al 100% | Yes |
| 6 | (Al) - NS | Arc Thermal Metal Spray | (Al) - (Al) [Single metal] | Al 100% | No |
| 7 | (Zn)-(Al) - S | Arc Thermal Metal Spray | (Zn) - (Al) [Single metal] | Zn 73%, Al 27% | Yes |
| 8 | (Zn)-(Al) - NS | Arc Thermal Metal Spray | (Zn) - (Al) [Single metal] | Zn 73%, Al 27% | No |
| 9 | (Zn-Sn) - S | Arc Thermal Metal Spray | (Zn-Sn) - (Zn-Sn) [Alloy] | Zn 65%, Sn 35% | Yes |
| 10 | (Zn-Sn) - NS | Arc Thermal Metal Spray | (Zn-Sn) - (Zn-Sn) [Alloy] | Zn 65%, Sn 35% | No |
| 11 | (Al-Mg) - S | Arc Thermal Metal Spray | (Al-Mg) - (Al-Mg) [Alloy] | Al 95%, Mg 5% | Yes |
| 12 | (Al-Mg) - NS | Arc Thermal Metal Spray | (Al-Mg) - (Al-Mg) [Alloy] | Al 95%, Mg 5% | No |

Substrate: SS41, 15 mm x 15 mm x 1.6 mm thickness; Experimental area: 0.78 cm²; Steel surface treatment: sand blast; Electrolyte solution: 3.5 wt. % NaCl; US¹: Unpainted Steel (Substrate); HDG²: Hot Dip Galvanizing (Zn 100%); Specimen Name³: (Type of spraying metal) - (S⁴: Pore sealing agent is sealed, NS⁵: Pore sealing agent is non-sealed)

2.3 Experimental procedures

Fig. 2 lists the steps for conducting the corrosion test of the ATMS film specimens. As shown in (a) and (b), ATMS was performed on the SS41 steel plate according to the metal wire type. In (c), a specimen was fixed to the exposure part of the corrosion test cell. The corrosion test cell was then filled with NaCl solution such that the specimen surface was completely immersed in the electrolyte, as shown in (d). In (e), the reference, working, and counter electrodes were connected to the corrosion test cell, and (f) shows the corrosion test cell connected to the potentiostat, which is the instrument used for measurement, for electrochemical impedance spectroscopy.

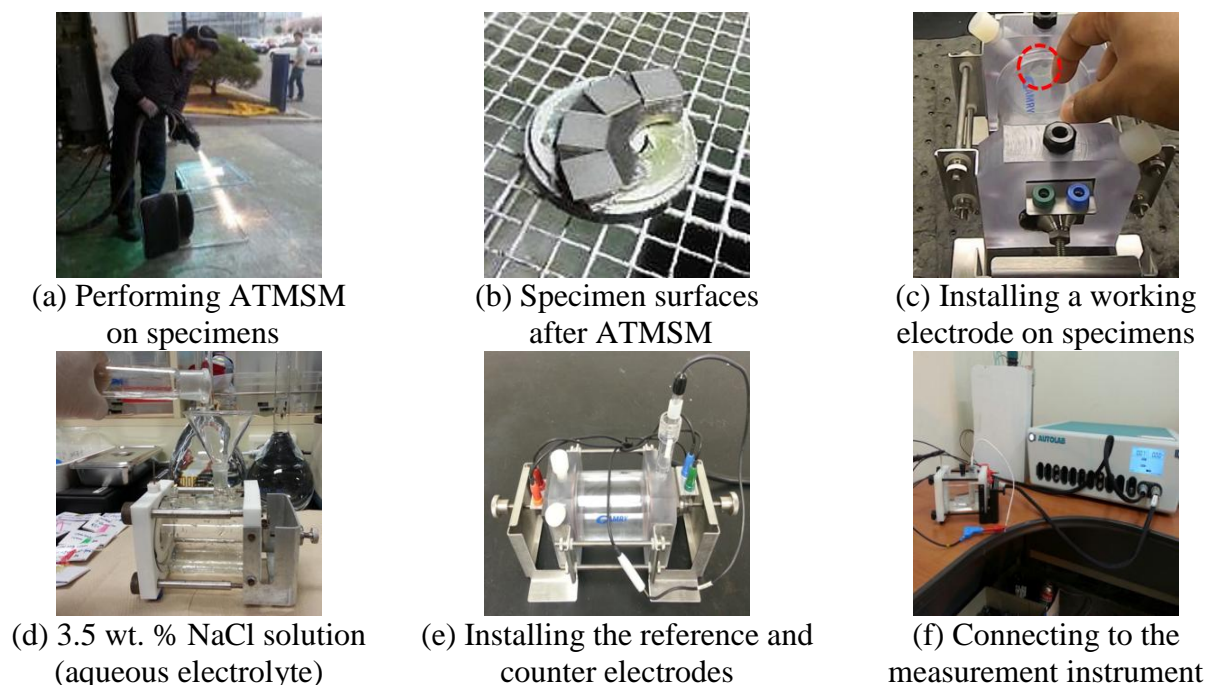


Figure 2. Steps for impedance spectroscopy measurement

Fig. 3 shows a schematic diagram of the experimental setup for electrochemical impedance spectroscopy. As indicated in Table 1, the dimensions of each specimen surface were $15 \text{ mm} \times 15 \text{ mm}$. A 3.5 wt. % NaCl solution was used to simulate seawater. The specimen area exposed to the solution for the measurement was configured to be a circle with a diameter of 1 cm (surface area: 0.78 cm^2). The specimen was used as the working electrode, and Platinum (Pt) and Ag/AgCl electrodes were used as the counter and reference electrodes, respectively.

PGSTAT 302N (Metrohm Autolab, KM Utrecht, Netherlands) was used as the instrument to measure impedance. The impedance values were measured in the frequency range of $10^5 - 10^{-1} \text{ Hz}$, thereby applying an AC voltage of $\pm 10 \text{ mV}$ to the specimens, based on measured open circuit potential (OCP). OCP is a self-potential which a specimen surface performs under the electrolyte, in the condition that there is no scanning of voltage or current. Because the application range of AC voltage

on the specimen should be appropriate to get accurate impedance value depending on each specimen, OCP of each specimen was firstly checked and AC voltage was applied.

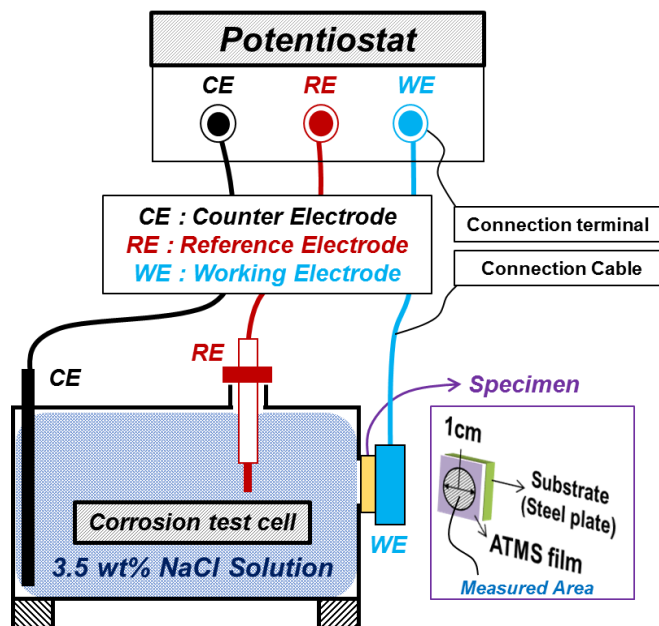


Figure 3. Schematic diagram of the experimental setup for electrochemical impedance spectroscopy

3. RESULTS AND DISCUSSION

3.1 Impedance comparison between conventional anti-corrosion films and non-sealed ATMS films

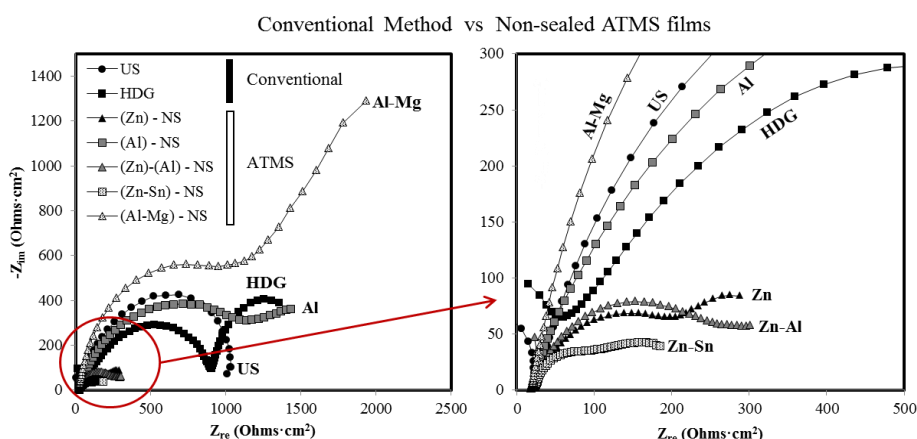


Figure 4. Impedance of the conventional anti-corrosion films and non-sealed ATMS films

Fig. 4 depicts the Nyquist plots showing the impedance of the conventional anti-corrosion films and non-sealed ATMS films. As can be seen in Fig. 4, the first semicircle observed for each test specimen is indicative of the charge transfer resistance at the interface between the electrolyte and ATMS film. The two conventional anti-corrosion films US and HDG exhibit a relatively high charge

transfer resistance than Zn series specimens (Zn, Zn–Al, Zn–Sn). Fig. 4 reveals that the electric charge transfer resistance of the ATMS films with different metal wire types follows the order of Al–Mg > Al > Zn–Al > Zn > Zn–Sn.

3.2 Impedance comparison between conventional anti-corrosion films and sealed ATMS films

Fig. 5 depicts the Nyquist plots showing the impedance of the conventional anti-corrosion films and sealed ATMS films. They demonstrate that the use of a pore sealing agent enhances charge transfer resistance; the Al–Mg ATMS film exhibits an effect greater than that exerted by other ATMS films. Even Zn and Zn–Al ATMS films which exhibited relatively lower charge transfer than US and HDG, they displayed similar high values of charge transfer resistance to Al ATMS film after the application of a pore sealing agent. By the application of the pore sealing agent, ATMS films exhibit higher values of charge transfer resistance than those of conventional anti-corrosion films (US, HDG).

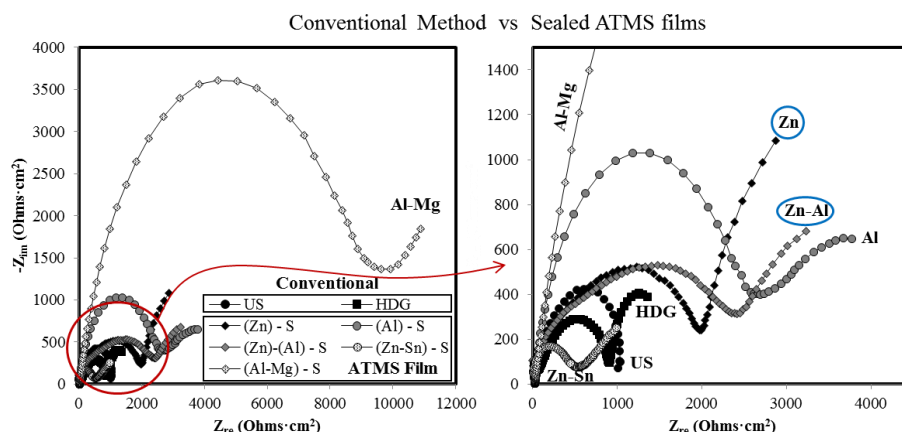


Figure 5. Impedance of the conventional anti-corrosion films and sealed ATMS films (Nyquist plots)

3.3 Impedance comparison between sealed and non-sealed ATMS films

Fig. 6 shows the Nyquist plots showing the impedance of the ATMS films under sealed and non-sealed conditions. The application of the pore sealing agent significantly improved the charge transfer resistance in all specimens regardless of the spraying metal types. By comparing the sealed and non-sealed Al and Al–Mg ATMS films, non-sealed Al and Al–Mg ATMS films have sufficient charge transfer resistance even without pore sealing agent.

These results suggest that Nyquist plots showing impedance provide intuitive information on the corrosion resistibility by the comparison and evaluation of individual specimens. However, the impedance values obtained from experiments do not yield an ideal semicircle. Therefore, it is essential to quantitatively represent the elements of impedance that are involved in a real reaction system, which are necessary for the design of an equivalent circuit and a fitting process. For this reason, an equivalent circuit for each specimen using Nova (Metrohm Autolab B. V., Netherlands), electrochemical impedance analysis software, was constructed to represent the impedances of the ATMS films with a

real reaction system for quantitative evaluation.

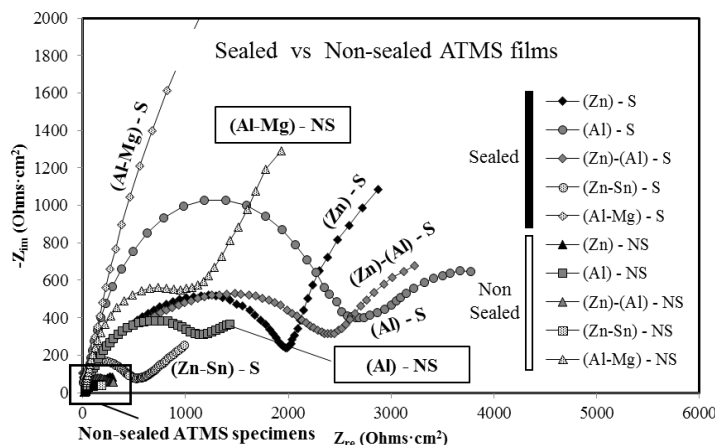


Figure 6. Impedance of the ATMS films under sealed and non-sealed conditions

Table 2 lists the whole impedance value of each specimen obtained by the design and fitting of the equivalent circuit. R_s , Y_0 -CPE1, and R_{ct} denote the electrolyte resistance, constant phase element (CPE) at the interface between the electrolyte and ATMS film, and charge transfer resistance of the ATMS film, respectively. Y_0 -CPE2 is the CPE between the ATMS film and substrate, and R_{Fe} denotes the resistance at the substrate. As individual components contributing to the impedance are not clearly distinguishable, impedance values are set by estimating the reactions at the interfaces assumed to occur in a real reaction system when designing equivalent circuits and performing fitting. Major reactions of each specimen as per its equivalent circuit can be identified by measuring the impedance value with the lowest estimated error (%) through fitting.

Table 2. Impedance value of each specimen obtained through its equivalent circuit design and fitting

| No | Specimen | R_s ($\Omega \cdot \text{cm}^2$) | Y_0 -CPE1 ($\mu\text{F}/\text{cm}^2$) | n- CPE1 | R_{ct} ($\Omega \cdot \text{cm}^2$) | Y_0 -CPE2 ($\mu\text{F}/\text{cm}^2$) | n- CPE2 | R_{Fe} ($\Omega \cdot \text{cm}^2$) | EC type |
|----|--------------|---|--|------------|--|--|------------|--|-----------------|
| 1 | US | 24.74 | 814.85 | 0.83 | 1082.30 | - | - | - | [R(QR)] |
| 2 | HDG | 42.68 | 3.74 | 0.73 | 834.19 | 1849.20 | 0.53 | - | [R(Q[RQ])] |
| 3 | (Zn)-S | - | 10.6 | 0.58 | 2039.10 | 1002.70 | 0.63 | - | (Q[RQ]) |
| 4 | (Zn)-NS | 22.92 | 502.89 | 0.78 | 129.41 | 6122.9 | 0.46 | 593.48 | [R(QR)(Q R)] |
| 5 | (Al)-S | 34.78 | 1.49 | 0.92 | 1999.10 | 682.70 | 0.24 | - | [R(Q[RQ])] |
| 6 | (Al)-NS | 20.75 | 61.4 | 0.73 | 1010.10 | 1908.7 | 0.34 | - | [R(Q[RQ])] |
| 7 | (Zn)-(Al)-S | - | 12.9 | 0.51 | 2371.70 | 1141.9 | 0.43 | - | (Q[RQ]) |
| 8 | (Zn)-(Al)-NS | 20.24 | 381.4 | 0.73 | 202.55 | 11868 | 0.35 | - | [R(QR)Q] |

| | | | | | | | | | |
|----|------------|-------|--------|------|---------|--------|------|--------|-------------|
| 9 | (Zn–Sn)–S | - | 1.17 | 0.78 | 418.45 | 1793.1 | 0.26 | - | [(QR)Q] |
| 10 | (Zn–Sn)–NS | 21.93 | 298.15 | 0.88 | 46.94 | 4388.5 | 0.48 | 205.37 | [R(QR)(QR)] |
| 11 | (Al–Mg)–S | - | 0.98 | 0.85 | 8668.60 | 268.26 | 0.39 | - | (Q[QR]) |
| 12 | (Al–Mg)–NS | - | 48.2 | 0.89 | 1114.20 | 834.92 | 0.59 | - | (Q[QR]) |

R_s : Solution Resistance; Y_0 -CPE1 : Constant Phase Element between electrolyte and interface of Anti-corrosion film; R_{ct} : Charge transfer resistance of Anti-corrosion Film; Y_0 -CPE2 : Constant Phase Element between Anti-corrosion film and substrate; R_{fe} : Resistance of Substrate;

EC type : Fitted equivalent circuit, Items between () are in parallel and [] are in series

3.4 R_s and R_{ct} of an ATMS film as per the composition of its equivalent circuit

R_s was measured in the range of 20–40 Ω . The sealed ATMS films exhibits values close to 0, presumably caused by the effect of pore sealing agent, which provides a stable protection for the ATMS film, resulting in a near-zero resistance toward the electrolyte.

In case of the comparison of the R_{ct} values of the non-sealed ATMS films, (Al–Mg)-NS exhibits the highest R_{ct} value, followed by Al, Zn–Al, Zn, and Zn–Sn; this order is in good agreement with that obtained by Nyquist plots. This implies that the Zn series metal type used as ATMS films induce an intensive sacrificial anodic reaction, resulting in relatively low initial charge transfer resistance of the ATMS films (Zn, Zn–Sn, and Zn–Al specimens). Likewise, the Al series ATMS films (Al, Al–Mg specimens) demonstrated a higher charge transfer resistance because of the superior corrosion resistant property of the Al metal, leading to efficient initial formation of oxidation film on the steel surface.

In case of the comparison of the R_{ct} values of the sealed ATMS films, the (Al–Mg)-S demonstrates an approximately 6-fold higher charge transfer resistance on average compared to other metal type ATMS films with pore sealing agent. It was found that quantitative comparison of the charge transfer resistance of the ATMS films by electrochemical impedance spectroscopy was possible and R_{ct} is the factor that determines the corrosion resistivity of the ATMS films.

These results indicate that the R_{ct} of the ATMS films significantly varies depending on whether the metal type applied pertains to the Zn or Al series. This variation may be explained by the fact that the anti-corrosion mechanisms of Zn and Al are different on the basis of the properties of the metals. However, the evaluation of the anti-corrosion performance by a comparison of the R_{ct} values of the ATMS films exhibited in the initial phase does not yield accurate values. To accurately evaluate the anti-corrosion performance of ATMS films according to metal type applied, it is necessary to analyze and compare the changes of impedance of the ATMS films in regards to being immersed in the electrolyte solution over a prolonged time period.

3.5 CPE of an ATMS film according to the composition of its equivalent circuit

Figs. 8–10 show the equivalent circuits of the ATMS films constructed for the analysis of the

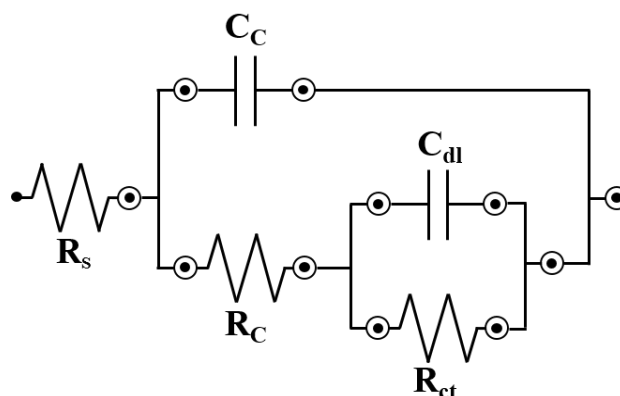
total reaction system of Zn, Zn-Al, and Al specimens and the results of subsequent fitting. The results show that the impedance curves after fitting are in good agreement with the measured data. Accordingly, a representative equivalent circuit that can explain the reaction system of the ATMS films was possible to be obtained.

One of the most important elements in the construction of the equivalent circuit of an ATMS film is the impedance called *CPE* (Constant Phase Element), which is an unprescribed part of the impedance conceived to explain the responses of a real reaction system. *CPE* is indispensable for analyzing the imperfect semicircle in the Nyquist plot. With *CPE*, the impedance element can be predicted from the value of n ; the closer the n value is to 1, 0.5, and 0, the more likely it is to exhibit the properties of capacitance's impedance, Warburg impedance, and resistance, respectively [16, 17].

In the case of Y_0 -CPE1 that appears at the interface between the electrolyte and ATMS film, n was measured to be close to 1, caused by the electric double layer that is formed at the interface of the ATMS film, presumably playing the role of a capacitance. Capacitance indicates the electric capacity required to accumulate electric charge. The lower the capacitance, the faster the accumulation of electric charge and the more difficult it is for the transfer of electric charge.

The Y_0 -CPE1 for sealed and non-sealed ATMS films was measured; the *CPE* values of the sealed ATMS specimens are found to be very low. From these results, it can be inferred that the pore sealing agent impedes the electric charge transfer at the interface of the ATMS film. For the reactions occurring between the ATMS film and Fe (= substrate), Y_0 -CPE2 was appeared in all specimens but resistance of substrate was not measured except for (Zn)-NS and (Zn-Sn)-NS).

Of the previous studies that have been reported about an equivalent circuit of the steel with anti-corrosion coating with porosity, a representative study has reported an equivalent circuit which shows resistance of coating with porosity (R_c), capacitance of coating (C_c), charge transfer resistance of substrate (R_{ct}) and capacitance of electric double layer between the anti-corrosion film and steel (C_{dl}) in the form of the AC circuit, as shown in Fig. 7 [18, 19]. In this study, however, the ATMS films investigated exhibit only Y_0 -CPE2, with n being close to 0.5, which is interpreted to exhibit Warburg impedance induced by diffusion.



R_s : Solution resistance; R_c : Resistance of coating with porosity; C_c : Capacitance of coating;
 R_{ct} : Charge transfer resistance of substrate (Fe); C_{dl} : Capacitance of electric double layer

Figure 7. A representative equivalent circuit of the substrate with an anti-corrosion coating (ISO 16773-4)

However, it is judged that this is not caused by diffusion reaction according to the penetration of electrolyte, instead it exhibits a property of galvanized metal due to the electrical contact between the ATMS film and steel; hence, the metal-to-metal electric charge transfer is considered to be active and work as an electric double layer. No corrosion was observed at the interface between the ATMS film and the substrate in our study probably because the test specimens consist of films in the pre-corrosion phase. This is also demonstrated by the finding that they have a larger capacitance as compared to Y₀-CPE1 [20, 21].

However, the specimens (Zn)-NS and (Zn-Sn)-NS exhibit resistance between the ATMS film and substrate (R_{Fe}). Hence, these specimens were evaluated to be ATMS films with relatively low anti-corrosion performance [9, 15]. This is assumed to be attributed to the insufficient charge transfer resistance of the ATMS film against the electrolyte to function as an anti-corrosion material, which can result in corrosion reactions between the steel and ATMS film. Such a high probability for corrosion is assumed to be attributed to the higher Y₀-CPE2 values compared with those of other ATMS films, which permit the accumulation of electric charge between two metals for each film [22].

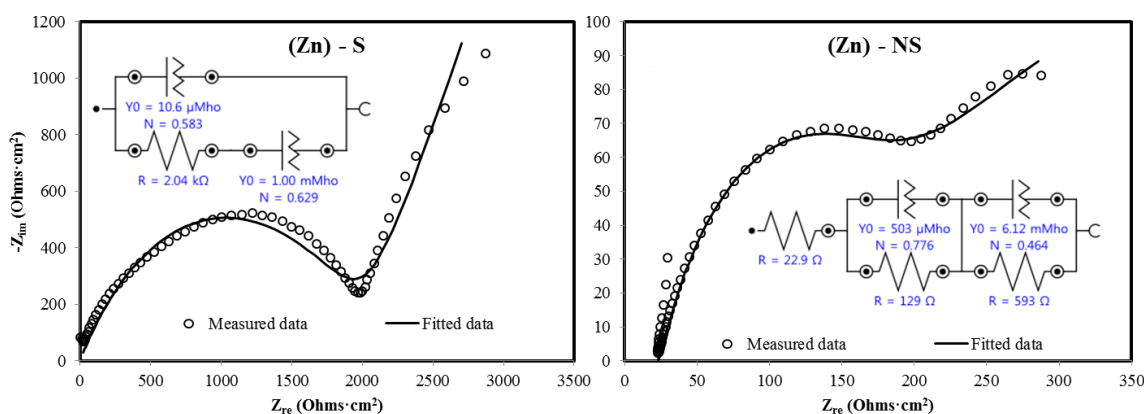


Figure 8. Equivalent circuit design and the result of fitting [(Zn)-S and (Zn)-NS]

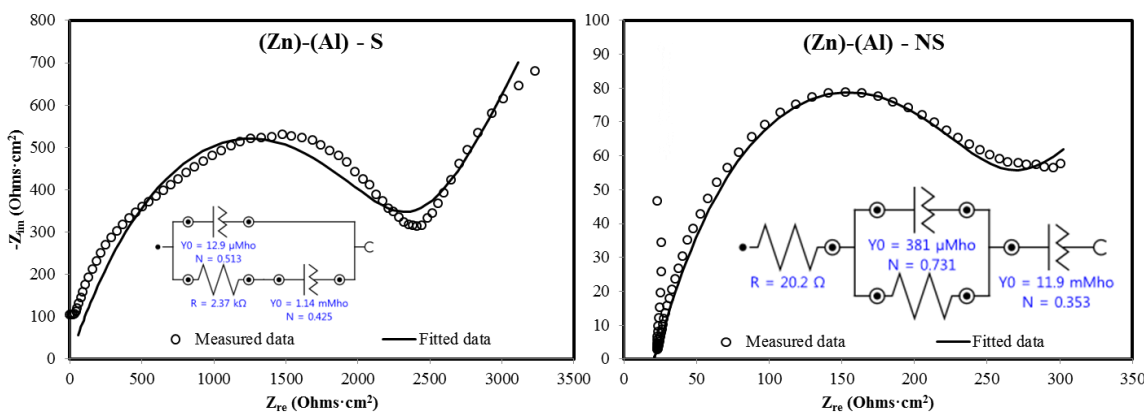


Figure 9. Equivalent circuit design and the result of fitting [(Zn)-(Al)-S and (Zn)-(Al)-NS]

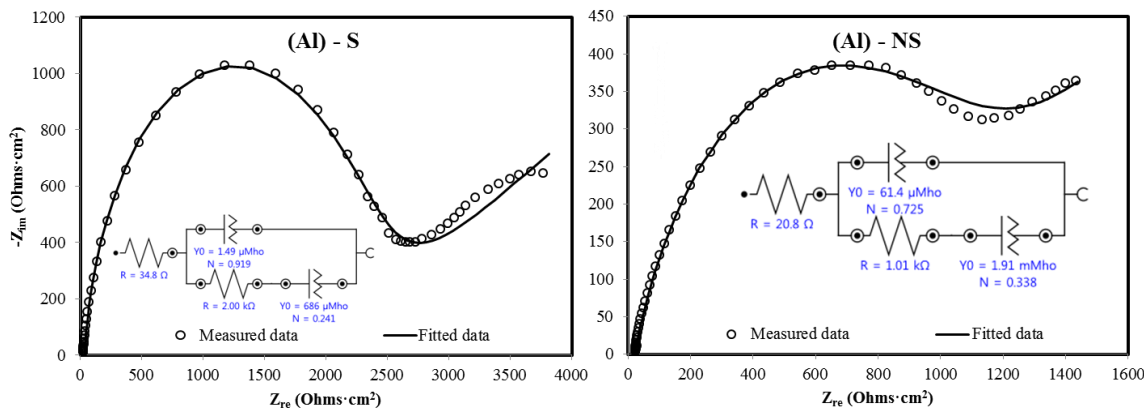


Figure 10. Equivalent circuit design and the result of fitting ((Al)-NS)

3.6 Representative equivalent circuits for the ATMS films according to anti-corrosion performance level

The reaction system of each specimen was analyzed by interpreting its equivalent circuit. It helped in the explanation of the reactions of ATMS films with three representative equivalent circuits, as shown in Figs. 11–13, respectively. Figs. 11 and 12 show the equivalent circuits for the specimens of the Zn-series ATMS films. Fig. 11 is the equivalent circuit [R(QR)(QR)] representing (Zn)-NS and (Zn-Sn)-NS, which exhibits the lowest anti-corrosion performance. This equivalent circuit shows resistance between the ATMS film and steel, which indicates that relatively rapid corrosion may occur when exposed to marine environments. Fig. 12 is the equivalent circuit [R(QR)Q] representing (Zn-Al)-NS and (Zn-Sn)-S, which probably demonstrates potential for a higher level of anti-corrosion performance than [R(QR)(QR)], but its high Y_0 -CPE2 value makes it vulnerable to corrosion caused by the high accumulation of electric charge between the ATMS film and steel. Fig. 13 is the equivalent circuit [R(Q[RQ])] representing the specimens for the Al-series ATMS films and those treated with a pore sealing agent. Previous studies have verified that the application of the Al-series metal type or a pore sealing agent enhances anti-corrosion performance [9, 15]. Consequently, it is judged that the ATMS films which can ensure excellent anti-corrosion performance are supposed to have the equivalent circuit [R(Q[RQ])] (Fig. 13). On the basis of the findings of this study, it was able to predict the total reaction system of ATMS films, the schematic diagram of which is shown in Fig. 14.

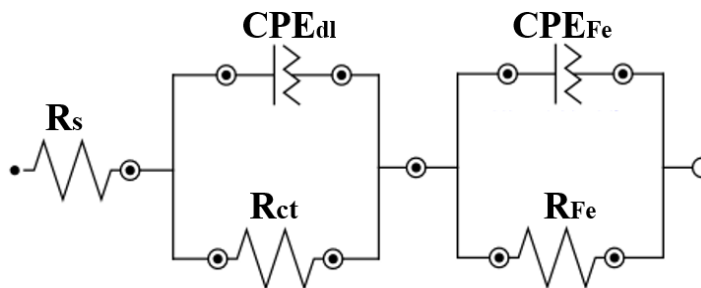


Figure 11. Equivalent circuit [R(QR)(QR)] representing the Zn-series ATMS films[(Zn-Sn)-NS, (Zn)-NS]

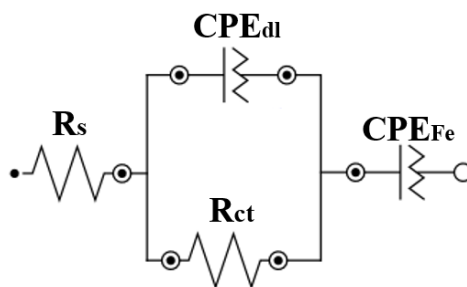


Figure 12. Equivalent circuit [R(QR)Q] representing the Zn-series ATMS films[(Zn-Sn)-S, (Zn-Al)-NS]

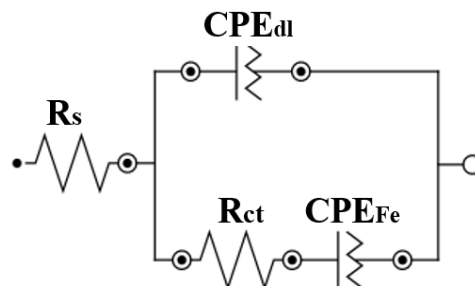


Figure 13. Equivalent circuit [R(Q[RQ])] representing the Al-series and sealed ATMS films[(Al-Mg)-NS, (Al)-NS, (Al-Mg)-S, (Al)-S, (Zn)-S, (Zn-Al)-S]

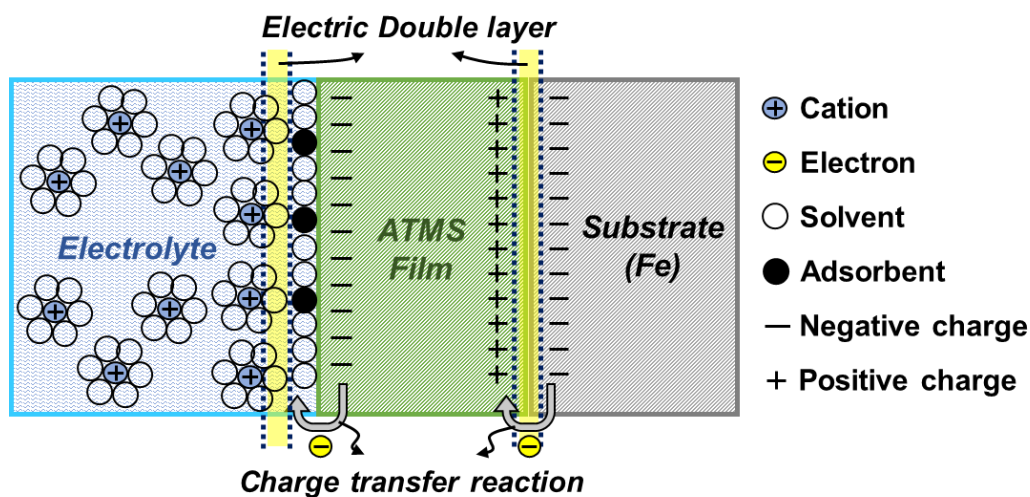


Figure 14. Schematic diagram of the predicted ATMS film reaction system in the electrolyte

4. CONCLUSIONS

This study analyzed the system of reactions that occur at the interface between the electrolyte and ATMS film by electrochemical impedance spectroscopy. The study also presented a representative equivalent circuit for ATMS film reactions by elucidating the elements conducive to corrosion resistivity depending on the interfacial conditions between ATMS films and substrates. As a result, the following conclusions could be drawn:

1. The measured electrolyte resistance (R_s) ranged between 20 and 40 Ω . However, the ATMS films treated with a pore sealing agent exhibited near-zero R_s values.

2. The charge transfer resistance (R_{ct}) of the ATMS films were quantitatively compared and evaluated by electrochemical impedance spectroscopy, which implies that R_{ct} is a factor determining the corrosion resistivity of ATMS films.

3. As a result of measuring the Y_0 -CPE1 depending on whether pore sealing agent was applied, it was found that sealed specimens exhibited very low CPE values. From this result, it can be inferred that the pore sealing agent hampers the transfer of electric charge at the interfaces of ATMS films.

4. By impedance measurements between the ATMS film and substrate (Fe), no resistance was mainly detected, Y_0 -CPE2 was measured. This may be explained by the property of galvanized metal induced by the electrical contact between the ATMS film and substrate, thus ensuring the active transfer of electric charge from metal to metal and work as an electric double layer.

5. Equivalent circuits representing ATMS films were obtained by modeling an equivalent circuit for each anti-corrosion film, and representative equivalent circuits were presented as models to be applied on ATMS film according to metal type (Zn series, Al series) and the presence or absence of a pore sealing agent.

ACKNOWLEDGMENTS

This research was supported by a grant (12-Advanced City-D02:13CHUD-C063720-02) from Construction Technology Research Program (CTRP) funded by Ministry of Land, Infrastructure and Transport (MLIT), Government of Republic of Korea.

References

1. V.D. Cocco, F. Iacoviello and S. Natali, *Theor. Appl. Fract. Mech.*, 70 (2014) 91.
2. T. Nishimura and V. Raman, *Materials*, 7 (2014) 4710.
3. S. Martinez, L.V. Zulj and F. Kapo, *Corros. Sci.*, 51 (2009) 2253.
4. S.G. Dong, B. Zhao, C.J. Lin, R.G. Du, R.G. Hu and G.X. Zhang, *Constr. Build. Mater.*, 28 (2012) 72.
5. T.S. Kim, H.S. Lee, J.H. Yoo, S.H. Tae, S.H. Oh, Y.C. Lim and S.B. Lee, *Mater. Manuf. Proc.*, 26 (2011) 14.
6. A. Guenbour, A. Benbachir and A. Kacemi, *Surf. Coat. Technol.*, 113 (1999) 36.
7. N. Cinca, C.R.C. Lima. and J.M. Guilemany, *J. Mater. Res. Technol.*, 2 (2013) 75.
8. D.F. Bettridge and R.G. Ubank, *Mater. Sci. Technol.*, 2 (1986) 232.
9. H.B. Choe, H.S. Lee and J.H. Shin, *Materials*, 7 (2014) 7722.
10. Y. Itoh, Y. Shimizu and A. Koyama, *J. JSCE A*, 63 (2007) 795.
11. A. Liu, *J. Univ. Sci. Technol. B*, 34 (2012) 1054.
12. M. Campo, M. Carboneras, M.D. Lopez, B. Torres, P. Rodrigo, E. Otero and J. Rams, *Surf. Coat Technol*, 203 (2009) 3224.
13. Q. Jiang, Q. Miao, W.P. Liang, F. Ying, F. Tong, Y. Xu, B.L. Ren, Z.J. Yao and P.Z. Zhang, *Electrochim. Acta*, 115 (2014) 644.
14. O. De Rincon, A. Rincon, M. Sanchez, N. Romero, O. Salas, R. Delgado, B. Lopez, J. Uruchutu, M. Marroco and Z. Panosian, *Constr. Build. Mater.*, 23 (2009) 1465.
15. H.S. Lee, M. A. Ismail and H. B. Choe, *Corros Rev*, 33 (2015) 31.
16. P. Córdoba-Torres, T.J. Mesquita, and R.P. Nogueira, *Electrochimica Acta*, 92 (2013) 323.

17. Y. Huang, H. Shih, and F. Mansfeld, *Materials and Corrosion*, 61 (2010) 302.
18. ISO 16773-4, Paints and varnishes - Electrochemical impedance spectroscopy (EIS) on high-impedance coated specimens - Part 4: Examples of spectra of polymer-coated specimens (2009).
19. C. Liu, Q. Bi, A. Leyland and A. Matthews, *Corrosion Science*, 45 (2003) 1243.
20. E.A. Esfahani, H. Salimijazi, M.A. Golozar, J. Mostaghimi and L. Pershin, *Journal of Thermal Spray Technology*, 21 (2012) 1195.
21. G.M. Treacy, G.D. Wilcox and M.O.W. Richardson, *Surface and Coatings Technology*, 114 (1999) 260.
22. Q. Jiang, Q. Miao, W.P. Liang, F. Ying, F. Tong, Y. Xu, B.L. Ren, Z.J. Yao, and P.Z. Zhang, *Electrochimica Acta*, 115 (2014) 644.

© 2015 The Authors. Published by ESG (www.electrochemsci.org). This article is an open access article distributed under the terms and conditions of the Creative Commons Attribution license (<http://creativecommons.org/licenses/by/4.0/>).